

LARGE DEFORMATION ANALYSIS OF FLEXIBLE MEMBRANE STRUCTURES AND THE EXPERIMENT

MASAHARU TOMIOKA^{*}, KATSUSHI IJIMA^{*} AND HIROYUKI OBIYA^{*}

^{*} Department of Civil Engineering and Architecture, Graduate School of Science and Engineering,
Saga University
1, Honjo, Saga, Japan
e-mail: ijimak@cc.saga-u.ac.jp

Key words: Orthotropic Membrane, Large Deformation, Compression-free, Experiment.

Summary. The paper proposes a method for analyzing large deformation of membrane structures. It is characteristic of the method to solve directly the equilibrium equations of forces working at the nodes in the structure. It is proved that the result of computing the large deformation behavior of a suspended membrane agrees well with the experimental result.

1 INTRODUCTION

The authors have been developing a method using a compression-free model suited to the characteristic of flexible membrane for analyzing large deformation of the structures^{1,2}. The method enables easy and stable computing any large deformation of the membrane from extremely slack state to tense state. There never occur multi-bifurcations in the computation because of using the compression-free model. Since the tension always exists in the membrane, the geometric stiffness makes the structure stable.

However, since the field of tension permits the areas of the elements composed the membrane to become zero, there are cases that the method gives impractical solutions according to a boundary condition. The most effective measure for preventing the element area from becoming zero is to consider the shear forces normal to the plane of the element.

The shear forces working at the apexes in the triangular element are balanced with the end moment derived from the bending moment in the side shared by the two elements. Although the method takes account of the bending moment, using the end shear forces prevents the increase of the degrees of freedom per node owing to take rotational that in. The idea has already proposed for shell problems^{3,4}, and the theory is being developed still⁵.

The paper clarifies that the geometric stiffness of the end shear forces resists the changes of the perpendicular lengths in the element. This effect of the geometric stiffness prevents zero area of the element.

Further, the paper shows the comparison of the experimental result and the computational that by the method. The experiment is the large deformation of the rectangular membrane suspended by fixing the two sides in opposition to each other.

2 ELEMENT END FORCES AND THE EQUILIBRIUM EQUATIONS

The method in the paper uses different procedure from that of the popular FEM. The strain energy of an element is defined by the positions of the nodes connected to the apexes of the element. In the method, the energy principal is applied to each element, and it gives the element end forces. The solution of the nodal positions is obtained from satisfying the equilibrium equation of the element end forces and the nodal forces at the nodal positions. The method is to use the two of the strain energies of the element in plane and out of plane.

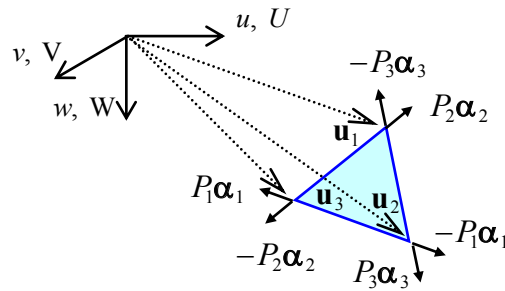


Figure 1: Element end forces in the plane

2.1 Element end forces in the plane

When the strain in a triangular element consisting a membrane structure are supposed to be uniform in the element, the element end forces can be defined as the forces parallel to the sides, shown in Figure 1.

When the position vectors of the three apexes in the element are \mathbf{u}_1 , \mathbf{u}_2 , \mathbf{u}_3 , the unit vectors expressing the directions of the three sides are,

$$\boldsymbol{\alpha}_1 = \frac{\mathbf{u}_3 - \mathbf{u}_2}{l_1}, \quad \boldsymbol{\alpha}_2 = \frac{\mathbf{u}_1 - \mathbf{u}_3}{l_2}, \quad \boldsymbol{\alpha}_3 = \frac{\mathbf{u}_2 - \mathbf{u}_1}{l_3}. \quad (1a, b, c)$$

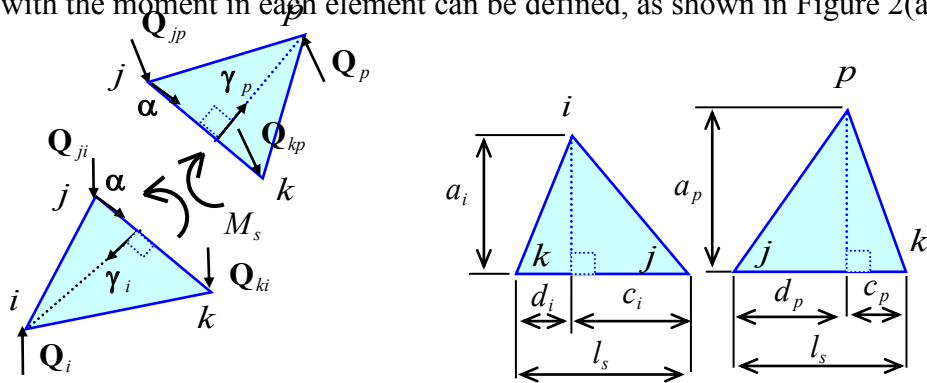
The nodal forces balanced with the element end forces are expressed by \mathbf{U}_1^{in} , \mathbf{U}_2^{in} , \mathbf{U}_3^{in} . The equilibrium equations at the three nodes connected to the three apexes are,

$$\begin{Bmatrix} \mathbf{U}_1^{\text{in}} \\ \mathbf{U}_2^{\text{in}} \\ \mathbf{U}_3^{\text{in}} \end{Bmatrix} = \begin{bmatrix} \mathbf{0} & \boldsymbol{\alpha}_2 & -\boldsymbol{\alpha}_3 \\ -\boldsymbol{\alpha}_1 & \mathbf{0} & \boldsymbol{\alpha}_3 \\ \boldsymbol{\alpha}_1 & -\boldsymbol{\alpha}_2 & \mathbf{0} \end{bmatrix} \begin{Bmatrix} P_1 \\ P_2 \\ P_3 \end{Bmatrix} = \mathbf{C}_e^{\text{in}} \mathbf{P}_e. \quad (2)$$

2.2 Element end forces out of the plane

The two elements of the element, ijk and the element, pkj share the side, jk and the bending moment, M_s occurring at the side is supposed to be uniform along the side.

When the moment, M_s works at each side, jk in the element, ijk and pkj , the end forces balanced with the moment in each element can be defined, as shown in Figure 2(a). The unit



(a) End shear forces balanced with the end moment

(b) Lengths in the two element

Figure 2: Element end forces out of the plane

vectors, \mathbf{n}_i and \mathbf{n}_p expressed by the following equations are the direction vectors normal to the planes of the two elements.

$$\mathbf{n}_i = \boldsymbol{\alpha} \times \boldsymbol{\gamma}_i, \quad \mathbf{n}_p = \boldsymbol{\gamma}_p \times \boldsymbol{\alpha}, \quad (3a, b)$$

where the unit vector, $\boldsymbol{\alpha}$ expresses the direction of the side, jk and the unit vectors, $\boldsymbol{\gamma}_i, \boldsymbol{\gamma}_p$ express the perpendiculars in the two elements, as shown in Figure 2.

The end forces expressed by using the lengths of the two elements shown by Figure 2(b) and the nodal forces, $\mathbf{U}_i^{\text{out}}, \mathbf{U}_j^{\text{out}}, \mathbf{U}_k^{\text{out}}, \mathbf{U}_p^{\text{out}}$ balancing at the four nodes give the equilibrium equations.

$$\begin{Bmatrix} \mathbf{U}_i^{\text{out}} \\ \mathbf{U}_j^{\text{out}} \\ \mathbf{U}_k^{\text{out}} \\ \mathbf{U}_p^{\text{out}} \end{Bmatrix} = \begin{Bmatrix} -\frac{\mathbf{n}_i}{a_i} \\ \frac{d_i \mathbf{n}_i}{a_i l_s} + \frac{c_p \mathbf{n}_p}{a_p l_s} \\ \frac{c_i \mathbf{n}_i}{a_i l_s} + \frac{d_p \mathbf{n}_p}{a_p l_s} \\ -\frac{\mathbf{n}_p}{a_p} \end{Bmatrix} M_s = \mathbf{C}_s^{\text{out}} M_s. \quad (4)$$

2.3 Equilibrium equations at the all of the nodes in the structure

When the force vector, \mathbf{U} represents the nodal forces working at the all of the nodes in the

structure, the equilibrium equation is,

$$\mathbf{U} = \sum_{e=1}^{m_e} \mathbf{C}_e^{\text{in}} \mathbf{P}_e + \sum_{s=1}^{m_s} \mathbf{C}_s^{\text{out}} M_s, \quad (5)$$

where m_e : the total number of the elements and m_s : the total number of the sides.

If the nodal forces and the element end forces do not balance, the equation (5) changes to,

$$\mathbf{U} - \sum_{e=1}^{m_e} \mathbf{C}_e^{\text{in}} \mathbf{P}_e - \sum_{s=1}^{m_s} \mathbf{C}_s^{\text{out}} M_s = \Delta \mathbf{U}. \quad (6)$$

We call $\Delta \mathbf{U}$ the unbalanced force vector. The method in the paper is to seek the nodal positions satisfying that the unbalanced forces at the all of the nodes are less than the allowable value.

3 COMPRESSION-FREE MODEL OF THE MEMBRANE ELEMENT

When the element is compression-free in the deformation in plane, and when the element end forces smoothly change together with the deformation, no matter how large deformation a membrane structure is, the phenomena can be easily and stably computed.

The deformation of the triangular element can be defined as the changes, $\Delta l_1, \Delta l_2, \Delta l_3$ from the lengths of the three sides, l_{10}, l_{20}, l_{30} in the non-stress element. The deformations of the side lengths are given with geometric exactitude from the nodal positions in Figure 1.

$$\begin{aligned} \Delta l_1 &= l_1 - l_{10} = \sqrt{(\mathbf{u}_3 - \mathbf{u}_2) \bullet (\mathbf{u}_3 - \mathbf{u}_2)} - l_{10} \\ \Delta l_2 &= l_2 - l_{20} = \sqrt{(\mathbf{u}_1 - \mathbf{u}_3) \bullet (\mathbf{u}_1 - \mathbf{u}_3)} - l_{20} . \\ \Delta l_3 &= l_3 - l_{30} = \sqrt{(\mathbf{u}_2 - \mathbf{u}_1) \bullet (\mathbf{u}_2 - \mathbf{u}_1)} - l_{30} \end{aligned} \quad (7)$$

When the strain in the element is supposed to be uniform, the relation between the element end forces, \mathbf{P}_e in the equation (2) and the deformations, $\Delta \mathbf{l}^T = \{\Delta l_1, \Delta l_2, \Delta l_3\}$ can be expressed by the following equation.

$$\mathbf{P}_e = \mathbf{k}_e \Delta \mathbf{l}. \quad (8)$$

The stiffness matrix, \mathbf{k}_e in the equation (8) is composed of the relation between the stress and the strain including the orthotropic characteristic, the direction of the fiber in the element and the element shape.

If the trussed unit in Figure 3(a) has the accurate stiffness per unit length of each axial member and the appropriate position of the sub-node, 4, the stiffness equation of the trussed unit is equivalent to the equation (8). The three of the axial members forming the same shape of the membrane element possess the stiffness per unit length, k_1, k_2 and k_3 . The three members connecting the sub-node with each apex are equivalent in the stiffness per unit

length, k_a . The position of the sub-node is determinable by the distances, h_1 , h_2 and h_3 from



(a) Trussed unit composed by 6 axial members (b) Axial forces expressed by the hyperbolic function

Figure 3: Trussed unit substituted for the uniform strain element

each side.

In order to provide the trussed unit with the compression-free quality, the hyperbolic function is applied to the relation between the axial forces in the trussed unit and the deformations, as shown in Figure 3(b). The hyperbolic function becomes determinate by the three conditions of the stiffness per unit length, k , the tension, N_0 to keep the measures in the non-stress element under the gravity and the deformation, $-\Delta l_c$ in the limit that the three apexes converge at a point. Using the trussed unit installed the hyperbolic axial force in makes easy and stable computing deformed phenomena from extremely relaxed state to tense state possible.

4 MODEL CONSIDERING BENDING RIGIDITY

Though the compression-free model makes the computation stable, unpractical solutions are sometimes derived as a result from assuming the compression-free. For example, when a plane membrane is suspended by a support of a part in the membrane under the gravity, the assumption derives the solution of the membrane shape deformed to a straight line that shows the total area of the membrane zero.

The most effective modifying the theory against the problem is to consider bending rigidity of membrane material. The bending rigidity of general membrane material is so small that the rigidity can be neglected. However, even if the bending moment in the membrane is a little, the geometric stiffness produced from the bending moment restricts the elastic deformation in the plane of the membrane. As a result, the method derives practical solutions and there is no phenomenon that the area of the membrane element becomes zero. Furthermore, the geometric stiffness does not induce the phenomena of multi-bifurcation to the process of the deformation, so that the computation is always stable.

The bending moment at the side, jk is derived as follows.

The four nodes in Figure 2 give the unit vectors, \mathbf{n}_i , \mathbf{n}_p normal to the two planes of the elements, as shown by the equations (3a, b). The cosine and the sine of the angle, θ between the two elements are,

$$\cos \theta = \mathbf{n}_i \bullet \mathbf{n}_p, \quad \sin \theta = \boldsymbol{\alpha} \bullet \mathbf{n}_i \times \mathbf{n}_p. \quad (9a, b)$$

When the angle between the two elements in non-stress is θ_0 , the changed angle by the bending deformation, $\Delta\theta$ is,

$$\Delta\theta = \theta - \theta_0. \quad (10)$$

When the two elements in Figure 2 are regarded as the two beams of the spans, a_{i0} and a_{p0} , that are the lengths of the perpendiculars in the two elements in non-stress, the widths of the two beams change from zero to the side length, l_s along the perpendiculars. Therefore, the curvatures induced by the end moment, M_s are uniform along the perpendiculars on the assumption that the deformations of the two beams are very small, and then the relation between the end moment, M_s and the changed angle, $\Delta\theta$ is,

$$M_s = \frac{2EI_s}{a_{i0} + a_{p0}} \Delta\theta, \quad (11)$$

where EI_s is the bending rigidity of the side, jk , and the value of the Young's modulus, E is to consider the direction of the fiber in the elements.

5 TANGENT STIFFNESS EQUATIONS INCLUDING GEOMETRIC STIFFNESS

The unbalanced forces are obtained from applying the element end forces, \mathbf{P}_e of the compression-free model and the end moments of the equation (11) to the equation (6). When the unbalanced force is over the allowable value, iterative methods of Newton-Raphson method or the method of dynamic relaxation using the tangent stiffness equation can easily reach convergent solutions.

The tangent stiffness equation is derived from differentiating the equilibrium equation (5), and the relation between the increment of the nodal forces, $\delta\mathbf{U}$ and the infinitesimal displacement, $\delta\mathbf{u}$ becomes the following.

$$\begin{aligned} \delta\mathbf{U} &= \sum_{e=1}^{m_e} (\delta\mathbf{C}_e^{\text{in}} \mathbf{P}_e + \mathbf{C}_e^{\text{in}} \delta\mathbf{P}_e) + \sum_{s=1}^{m_s} (\delta\mathbf{C}_s^{\text{out}} M_s + \mathbf{C}_s^{\text{out}} \delta M_s) \\ &= (\mathbf{K}_G^{\text{in}} + \mathbf{K}_O^{\text{in}}) \delta\mathbf{u} + (\mathbf{K}_G^{\text{out}} + \mathbf{K}_O^{\text{out}}) \delta\mathbf{u}, \end{aligned} \quad (12)$$

where \mathbf{K}_G^{in} : the geometric stiffness originating from the end forces, \mathbf{P}_e , \mathbf{K}_O^{in} : the stiffness relating to the elastic rigidity of the membrane, $\mathbf{K}_G^{\text{out}}$: the geometric stiffness originating from the end moment at the element side, $\mathbf{K}_O^{\text{out}}$: the stiffness relating to the bending rigidity of the membrane material. \mathbf{K}_G^{in} resists only the deformation out of the membrane, \mathbf{K}_O^{in} resists only the elongation of the membrane and $\mathbf{K}_O^{\text{out}}$ resists only the bending deformation.

The stiffness resistant to shrink of the membrane is included in only the stiffness of $\mathbf{K}_G^{\text{out}}$. When $\delta\mathbf{C}_s^{\text{out}} M_s$ is definitely expressed, it becomes clear that the end share forces balancing the end moment produce the stiffness resistant to the shrink of the element.

Differentiating $\mathbf{U}_i^{\text{out}}$ in the equation (4) gives

$$\begin{aligned} \delta\mathbf{U}_i^{\text{out}} = & \frac{M_s \mathbf{n}_i}{a_i^2} \left\{ \frac{c_i}{l_s} \boldsymbol{\gamma}_i^T (\delta\mathbf{u}_i - \delta\mathbf{u}_k) + \frac{d_i}{l_s} \boldsymbol{\gamma}_i^T (\delta\mathbf{u}_i - \delta\mathbf{u}_j) \right\} \\ & + \frac{M_s}{a_i^2 l_s} \left\{ (a_i \boldsymbol{\alpha} - c_i \boldsymbol{\gamma}_i) \mathbf{n}_i^T \delta\mathbf{u}_k - (a_i \boldsymbol{\alpha} + d_i \boldsymbol{\gamma}_i) \mathbf{n}_i^T \delta\mathbf{u}_j \right\}, \end{aligned} \quad (13)$$

where $\delta\mathbf{u}_i$, $\delta\mathbf{u}_j$, and $\delta\mathbf{u}_k$ are the infinitesimal displacement of the three nodes connecting the three apexes in the element, ijk in Figure 2.

The first term of $\left\{ c_i \boldsymbol{\gamma}_i^T (\delta\mathbf{u}_i - \delta\mathbf{u}_k) + d_i \boldsymbol{\gamma}_i^T (\delta\mathbf{u}_i - \delta\mathbf{u}_j) \right\} / l_s$ in the equation (13) is the infinitesimal increment of the perpendicular vector: $a_i \boldsymbol{\gamma}_i$ caused by the infinitesimal displacements of the three nodes, and $M_s \mathbf{n}_i / a_i = -\mathbf{Q}_i$ is the end shear force working the node, i . Therefore, the first term indicates that the end shear force resists shrinkable deformation or elongate one of the perpendicular in the plane of the element. Incidentally, the second term in the equation (13) expresses the resistant forces against the displacement component normal to the plane.

6 EXPERIMENT AND DISCUSSIONS

The theory in the method uses the compression-free assumption for analyzing the large deformation of membrane structures because the assumption makes the computation stable. However, it is not clear whether the assumption can be applied to real membrane. The following experiment of measuring large deformation of flexible membrane shows the validity of the assumption and the application of the theory to the analysis.

6.1 Measuring test for material constants of membrane

The membrane called Tarpaulin Super Green used in the experiment consists of nylon fabric coated with polyvinyl chloride. Naturally, the membrane is orthotropic. The test of elongating the rectangle specimen was conducted, as shown in Figure 4, in order to obtain the material constants. The membrane material is too soft to measure exactly the strain by using any strain gage. This is particularly why the adhesive to attach the strain gages to the membrane were stiffer than the membrane. Therefore, the strain gages: KFEN-2-120-C1L1M2R KYOWA was used only to obtain the Poisson ratio, and the laser displacement transducer: Model 3625 Yokogawa Electric Corporation in Figure 4 was used to obtain the Young's modulus. The strain gages could not measure exact strain, but the ratio of the two strains right-angled each other was expectantly accounted constant and the consideration seemed valid.

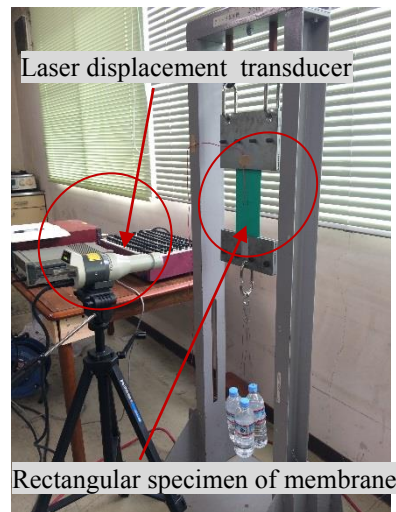


Figure 4: Test for measuring material constants

Essentially and naturally, a fabric has the characteristic that the material constants in the two directions of the fibers interact each other following the tense states of the fibers. However, in this experiment, the interaction did not need to be considered because so much tension did not occur in the membrane.

The material constants obtained were the weight per area: 4.59 N/m^2 , the elongation stiffness: $E_u t = 217.717 \text{ kN/m}$ and $E_v t = 80.785 \text{ kN/m}$ and the Poisson ratio: $\nu_u = 0.1638$ and $\nu_v = 0.0608$, where u and v were the directions of the warp and the weft in the respective fibers, and t was the thickness of the membrane.

6.2 Comparison of the experimental results and the computation

The experiment was to measure the deformation of the rectangular membrane of 1.1m in length and 0.5m in width suspended by fixing the two sides with the span of 0.96m. The deformation was given by raising the middle point in the free side in the membrane, as shown in Figure 5(a). Figure 5(a) is the deformation by raising the point from the vertical position of 0.126m to -0.05m in the w axis. The w axis is the direction of the gravity and $w=0$ is at the level of the fixed sides. Figure 5(b) is the deformation computed on the same condition of the raising. The membrane in the computation consists of 880 elements and the allowable unbalanced force is 0.0001N. The two figures as a whole show similar deformation each other.

The experiment was to measure the positions of the markers shown in Figure 5(a) by using a surveying instrument. Figure 6 shows the positions in the v - w coordinates by raising the point at the vertical position of -0.05m and -0.138m. The v axis is the horizontal line from the raised point to the middle point in the free side. The computational results agree well with the experimental results.

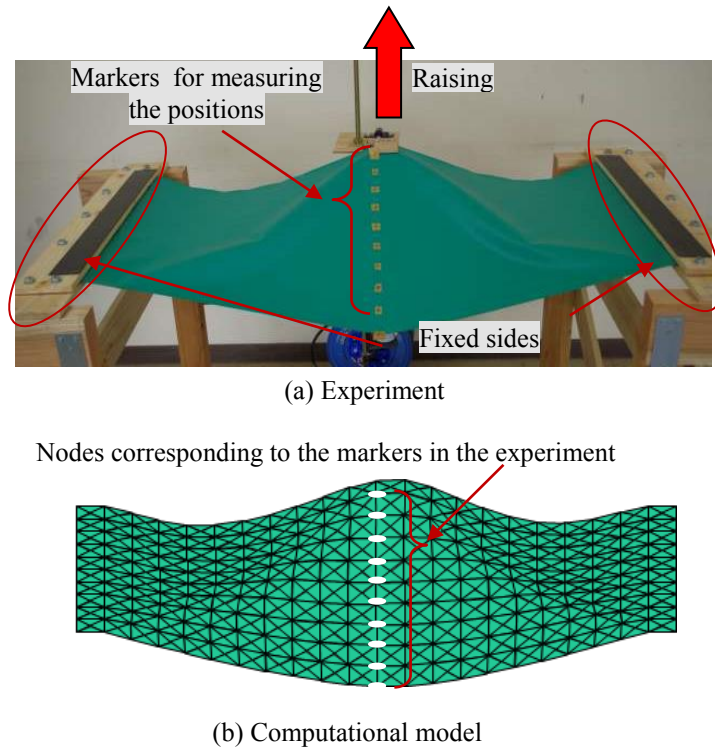


Figure 5: Large deformation of the suspended membrane

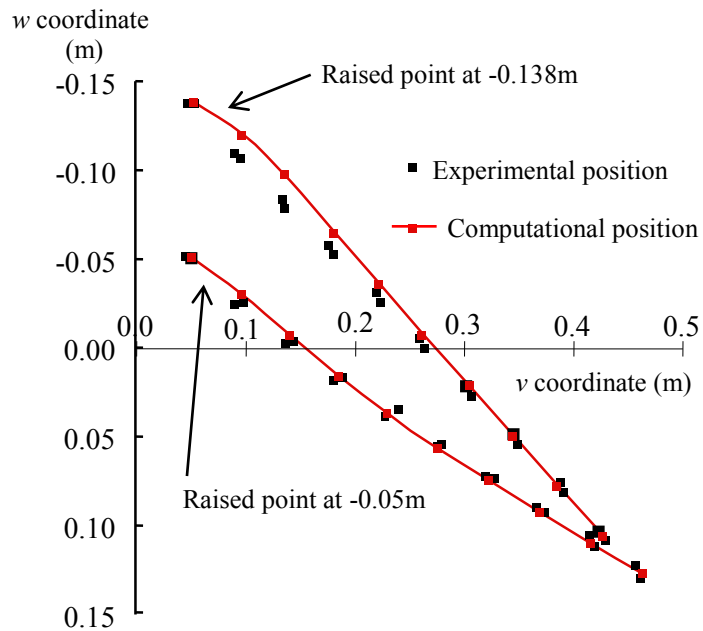


Figure 6: Positions of markers in the experiment and the computational positions

7 CONCLUSIONS

- The method proposed in the paper for analyzing large deformations of membrane structures is directly to solve the equilibrium equations at the all nodes in the structure. The equilibrium equations consist of the element end forces in the compression-free model, the end shear forces out of the plane of the membrane caused by the bending rigidity and the external forces working at the nodes.
- Though the end shear forces are very small because of the flexibility of membrane, the end shear forces resist the deformation in the plane of the membrane. Therefore, considering the end shear forces corrects impractical solutions by using only the compression-free model. The resistance resulting from the end shear forces is clearly shown by the geometric stiffness derived in the paper. Furthermore, the end shear forces do not bring multi-bifurcations into the method, but more stable computations.
- The validity of using the compression-free model and the reliability of the end shear forces is discussed with experimenting the large deformation of a suspended membrane. The theoretical values by the method agree well with the experimental values.

REFERENCES

- [1] Ijima K., Obiya H. and Kawasaki N. Large displacement analysis of compression-free membrane structures replaced by elastic cable units. *Int. Conf. on Textile Composites and Inflatable Structures, STRUCTURAL MEMBRANES 2009*. on CD-ROM, (2009).
- [2] Ijima K., Obiya H. and Kido K. An orthotropic membrane model replaced with line-members and the large deformation analysis. *Int. Conf. on Textile Composites and Inflatable Structures, STRUCTURAL MEMBRANES 2011*. on CD-ROM, (2011).
- [3] Phaal R. and Calladine CR. A simple class of finite elements for plate shell problems. II: An element for thin shells with only translational degrees of freedom. *Int. J. Numer. Meth. Engng.* 5:979-996, (1992).
- [4] Oñate E. and Cervera M. Derivation of thin plate bending elements with one degree of freedom per node. *Engineering Computations.* 10:553-561, (1993).
- [5] Flores F. G. and Oñate E. A rotation-free shell triangle for the analysis of kinked and branching shells. *Int. J. Numer. Meth. Engng.* 69:1521-1551, (2007).